Cholesterol Level Regulates Endosome Motility via Rab Proteins

Hongtao Chen,* Jun Yang,* Philip S. Low,*[†] and Ji-Xin Cheng*[†][‡]
*Department of Chemistry, [†]Purdue Cancer Center, and [‡]Weldon School of Biomedical Engineering, Purdue University,
West Lafayette, Indiana 47907

ABSTRACT   The role of cholesterol in the regulation of endosome motility was investigated by monitoring the intracellular trafficking of endocytosed folate receptors (FRs) labeled with fluorescent folate conjugates. Real-time fluorescence imaging of HeLa cells transfected with green fluorescent protein-tubulin revealed that FR-containing endosomes migrate along microtubules. Moreover, microinjection with antibodies that inhibit microtubule-associated motor proteins demonstrated that dynein and kinesin I participate in the delivery of FR-containing endosomes to the perinuclear area and plasma membrane, respectively. Further, single-particle tracking analysis revealed bidirectional motions of FR endosomes, mediated by dynein and kinesin motors associated with the same endosome. These experimental tools allowed us to use FR-containing endosomes to evaluate the impact of cholesterol on intracellular membrane trafficking. Lowering plasma membrane cholesterol by metabolic depletion or methyl-β-cyclodextrin extraction was found to both increase FR-containing endosome motility and change endosome distribution from colocalization with Rab7 to colocalization with Rab4. These data provide evidence that cholesterol regulates intracellular membrane trafficking via modulation of the distribution of low molecular weight G-proteins that are adaptors for microtubule motors.

INTRODUCTION

Endocytosis constitutes a major pathway for the delivery of membrane components, ligands, and solute molecules to various destinations inside eukaryotic cells (1). After internalization, endocytosed materials first appear in the peripheral cytoplasm, normally in early endosomes. From there, internalized molecules can be recycled back to the cell surface or selectively delivered to recycling endosomes or late endosomes for further transport and degradation. This complicated intracellular transport process is well regulated. Nevertheless, how a cell controls endosomal transport has not yet been fully clarified.

It has been suggested that cholesterol plays an important role in intracellular transport (2). Normally, cholesterol is found in the plasma membrane and early endosomes and is sorted away from late endosomes and lysosomes (3). Recent studies have further revealed that cholesterol is not a passive component of endosomal membranes, but rather is directly involved in the sorting and transport of endocytic vesicles (4). Thus, cholesterol content has been shown to affect the sorting of endocytosed lipid probes and glycosylphosphatidylinositol (GPI)-anchored proteins (5–7). In Niemann-Pick C disease, missorting of cholesterol by the dysfunctional NPC1 protein leads to cholesterol accumulation in late endocytic vesicles and subsequent inhibition of vesicle trafficking along microtubules (MTs) (8,9). Cholesterol also appears to be involved in the targeting of glycosphingolipids, as evidenced by their abnormal intracellular sorting and accumulation in late endosomes of cells from patients with sphingolipid storage diseases. It has been suggested that sphingolipid accumulation in sphingolipid storage disease cells induces cholesterol redistribution, which in turn perturbs the intracellular trafficking of glycosphingolipids, leading to their altered distribution (10).

A special form of receptor-mediated endocytosis involving the folate receptor (FR) (11–13) provides a unique system for assessing the role of cholesterol and sphingolipids in the intracellular transport of endocytic vesicles. Both FR α and FR β are GPI-anchored proteins that lack membrane-spanning and cytoplasmic domains normally required for docking to endocytic machinery. Instead, FR is associated with lipid rafts (14), which are enriched in cholesterol and sphingolipids (15). Therefore, the study of its endocytic machinery allows us to investigate the functions of lipids in endocytic trafficking (13).

The mechanisms underlying FR-mediated endocytosis have been extensively explored. FR internalization has been shown to be clathrin independent (16). Although it was initially thought that FR might be associated with caveolae and internalized via the pinching off of caveolae in a process called potocytosis (17), subsequent investigations have suggested that FRs are diffusely distributed over the plasma membrane and only clustered in caveolae upon cross-linking (18,19). Further studies have shown that FR resides in lipid rafts through its GPI anchor (14) and that the GPI anchor is essential for FR endocytosis. For instance, replacing the GPI anchor with the transmembrane domain and cytoplasmic tail of the low-density lipoprotein receptor leads to delivery of FRs to clathrin-coated pits (20). More recently, Mayor and co-workers have demonstrated that FRs are internalized into

a GPI-anchored protein-enriched early endosomal compartment via a clathrin- and caveolae-independent pinocytic pathway (21).

After internalization, FR-containing endosomes (referred as to FR endosomes in the rest of this work) are delivered to an endocytic recycling compartment (ERC) in FR-transfected Chinese hamster ovary (CHO) cells (22) or a peri-Golgi region in KB cells (23,24). In KB, HeLa, IGROV, M109, HS578T, MDA231 (25,26), MA104 (11), CHO, and Cos-7 cells (21), endocytosed FRs have been shown to be partially recycled back to the plasma membrane. The role of lipids in this internalization and recycling has been investigated by several groups. In MA104 cells, it was shown that cholesterol depletion increases the ratio of the external FR to internal FR pool (12). In another work, Maxfield and co-workers showed that the recycling of GPI-anchored proteins is three times slower than the recycling of other membrane components (22). However, this recycling rate could be increased by the depletion of cholesterol or sphingolipids or by replacing the GPI anchor with a transmembrane protein sequence (27). Nevertheless, the mechanism underlying the delivery of FR endosomes to ERC and back to the plasma membrane is still not fully understood.

To explore the machinery involved in intracellular FR transport and the role of cholesterol in FR recycling, we employed real-time imaging to study the intracellular trafficking of single FR endosomes in KB and HeLa cells. Using a HeLa cell line transfected with green fluorescent protein (GFP)-tubulin, bidirectional movement of FR endosomes along MTs is directly visualized. Further, we show that dynein and kinesin I motor proteins participate in the delivery of FR endosomes toward the MT minus and plus ends, respectively. Moreover, through single-particle tracking (SPT) (28,29) analysis, we provide evidence that lowering cholesterol enhances the motility of FR endosomes. Finally, we show that such regulation is accomplished via Rab7 and Rab4 GTPases.

MATERIALS AND METHODS

Chemicals and plasmids

Folate rhodamine (F-Rh) was synthesized using Fmoc (9-fluorenylmethyl carbamate) peptide chemistry. Folate-deficient medium RPMI 1640, pen-icillin-streptomycin, Amplex Red cholesterol assay kit, BODIPY-FL ceramide-bovine serum albumin (BSA), LysoTracker Yellow HCK-123, and transferrin rhodamine were purchased from Invitrogen (Carlsbad, CA). Fetal bovine serum, colchicine, nocodazole, compactin, mevalonate, and bicinchoninic acid (BCA) protein assay reagent kit were obtained from Sigma (St. Louis, MO). Dynein intermediate chain antibody (MAB1618) and kinesin I heavy chain antibody (MAB1613) were purchased from Chemicon (Temecula, CA). FuGENE 6 transfection reagent was purchased from Roche (Indianapolis, IN). GFP-Rab7 and the dominant-negative version of GFP-Rab7 were gifts from Dr. Jean Gruenberg (University of Geneva, Switzerland). GFP-Rab4 and GFP-Rab11 were gifts from Dr. Marino Zerial (Max Planck Institute, Germany). Mouse anti-p150[Glued] and cy2-labeled secondary antibody were purchased from BD Biosciences (San Jose, CA). Paclitaxel (PTX) was provided by SamYang Ltd. (Seoul, Korea).

Cell culture

KB cells expressing FR-α were obtained from American Type Culture Collection. A GFP-tubulin stably transfected HeLa cell line expressing FR-α was a kind gift from Xiaoqi Liu. All cell lines were cultured at 37°C in a humidified atmosphere containing 5% CO_2 and grown continuously in folate-deficient RPMI 1640 medium supplemented with 10% fetal bovine serum (FBS), 100 unit/ml penicillin, and 100 μg/ml streptomycin.

Coverslip-bottomed petri dishes (MatTek, Ashland, MA) were used for high-resolution imaging. Before each experiment, 6×10^4 cells in 1 ml growth medium were deposited into a petri dish and incubated for 3–4 days to encourage adherence and cell confluence. To label the FR, cells were incubated with 50 nM fluorescent folate conjugates at 0°C for 1 h or at 37°C for 30 min, as indicated in different experiments. Nonspecifically bound folate conjugate was removed by washing $3\times$ with fresh medium. Transient transfection of KB cells with Rab protein plasmid was carried out by following the instructions of FuGENE 6.

Treatment of cells with microtubule perturbants and motor protein antibodies

To disrupt MTs, cells were incubated for 2 h at 37°C with 10 μM (final concentration) colchicine or nocodazole before labeling with F-Rh for 30 min. The cells were then incubated for 3.5 h before imaging. Growth medium supplemented with low (60 nM) or high (10 μM) concentrations of paclitaxel (PTX) was used to stabilize or redistribute the MT network, respectively (30). After F-Rh labeling, the cells were incubated for 3.5 h at 37°C to allow sufficient FR internalization. The cells were then incubated with 60 nM PTX for 30 min to stabilize the MTs or incubated with 10 μM PTX for 30 min to redistribute the MT network before imaging. To examine the role of cytoplasmic dynein and kinesin I in FR trafficking, cells were microinjected with anti-dynein antibody or anti-kinesin I antibody at 1 mg/mL loading concentration.

Confocal fluorescence imaging

Cells were imaged on an IX70 inverted microscope (Olympus, Tokyo, Japan) equipped with a FV300 scanning unit and a 60$\times$ water-immersion objective (numerical aperture 1.2). A 543-nm HeNe (helium-neon) laser was used to excite F-Rh and transferrin rhodamine. A 488-nm Ar$^+$ laser was used to excite GFP and BODIPY-FL. The typical laser power at the sample was $\sim$80 μW. Images of 512 $\times$ 512 pixels were acquired at 2.7 s per frame. Movies of the area of interest were recorded for 30 s at a speed of 2–3 frames per second with a pixel size of from 90 to 150 nm. During the 30-s recording, $\sim$25% fluorescence bleaching occurred, which did not affect the analysis of SPT. FluoView software (Olympus) was used to convert each movie to a series of 8-bit tagged image file format files for SPT analysis.

Single-particle tracking analysis

A detailed description of the SPT method can be found elsewhere (31). We modified a code written by the Interactive Data Language to track various ''Gaussian-like'' blobs which mimic the spherical fluorescent endosomes moving in live cells. The suitable diameter for the tracking of the blobs (or endosomes) is between 5 and 20 pixels. The image pixel sizes were carefully adjusted to meet this requirement.

The analysis procedure is briefly described below. FR endosomes in each movie frame were identified based on size, total and mean fluorescence intensity, and eccentricity. The center position of an endosome was determined at subpixel resolution by fitting its fluorescence intensity profile to a Gaussian profile. The positions of the same endosome in adjacent frames were connected to plot the trajectory of this endosome. The instantaneous velocity was calculated as the displacement divided by the time interval between two adjacent frames. Plus and minus velocities were used to

indicate movements toward the cell periphery, i.e., the MT plus end, and the MT organizing center (MTOC), i.e., the MT minus end, respectively. The trajectory length was calculated as a summation of movements at each time internal. The laser was focused on a plane 5 μm above the lower surface of the cell. This plane was well separated from the top surface and bottom of the cell, which allowed facile visualization of the trafficking of FR endosomes between ERC and the plasma membrane. Because some endosomes moved into a different focal plane and disappeared from the movie, a time length threshold of 10 s was used to discard the short trajectories.

Mean-square displacement (MSD) analysis was conducted to identify the trafficking modes. The MSD was calculated as a function of the lag time (Δt) for lags <3/4 of the total trafficking time (28). The MSD curve was fitted on the basis of the following equations:

$$\mathrm{MSD}(\Delta t) = 4D\Delta t + (v\Delta t)^2, \qquad (1)$$

where D is the diffusion coefficient and v is the average velocity. Equation 1 describes diffusion (first part) plus directed motion (second part), which represents the active transport of endosomes inside of cells.

To evaluate the perturbations due to mechanical drifting in the setup and fluctuations of the fluorescence intensity profile, we measured the position fluctuations of rhodamine aggregates fixed on a coverslip. These aggregates produced the same fluorescence intensity as the FR endosomes. The instantaneous velocities of the fixed dots were measured to be <0.12 μm/s. Their positions could be determined with a standard deviation of <40 nm. Such stability allowed us to determine the endosome position with subpixel precision.

Cholesterol depletion and assay

For the metabolic depletion of cellular cholesterol, cells were grown for the desired period of time in 5% lipoprotein-deficient serum supplemented with 250 μM mevalonate and 10 μM compactin (22). For acute extraction of plasma membrane cholesterol, cells were incubated with 5 mM MβCD at 37°C for 30 min (14). Cholesterol levels were measured by an Amplex Red cholesterol assay kit according to the manufacturer's instruction and normalized by protein levels measured with a BCA protein assay reagent kit.

Measurement of FR recycling by autoradiography

KB cells were first incubated with 100 nM free folic acid at 0°C for 1 h to saturate all FRs on the cell surface. After washing with phosphate buffer saline (PBS) to remove unbound folic acid, cells were incubated with 30 nM [^{3}H]folic acid at 37°C for various lengths of time. The free [^{3}H]folic acid in the culture medium was then removed, and the cells were lysed with sodium hydroxide. The radioactivity of the cell lysates was measured by a Packard 1600CA liquid scintillation analyzer (Meriden, CT). The recycling rate k_e was calculated by fitting the increase of radioactivity (I_f) versus the [^{3}H]folic acid incubation time (t) with an exponential model (32):

$$I_f = A[1 - \exp(-k_e \times t)], \qquad (2)$$

where A is a constant and k_e represent the recycling rate. $T_{1/2}$ is calculated as $0.693/k_e$.

Immunofluorescence

KB cells were incubated with 50 nM fluorescent F-Rh at 37°C for 30 min followed by 3× washing with fresh medium. After 2 h incubation, cells were fixed with 3.7% formaldehyde in PBS for 20 min and permeabilized for 5 min with 0.05% Triton X-100 in PBS. Nonspecific binding of antibodies was blocked by 1% BSA in PBS for 1 h. Bound primary antibodies were visualized with cy2-labeled secondary antibody.

RESULTS

As a prelude to characterizing the role of cholesterol in FR vesicle trafficking, we first mapped the intracellular itinerary of endocytosed FR using folate-linked fluorescent dyes that bind with nanomolar affinity to the FR. We also analyzed the motility of FR endosome using SPT. The results are described below.

FR endosomes are delivered to ERC along microtubules

In KB cells labeled with F-Rh (F-Rh, red), FR endosomes were seen to traffic initially to a region of the perinuclear cytoplasm that was largely devoid of Golgi apparatus (see Fig. 1 A, green). This region was then shown to include the endosome recycling center (ERC), because analogous experiments with KB cells labeled simultaneously with folate BODIPY-FL and transferrin rhodamine (used as a marker of the ERC (33)) showed that after 30 min of coadministration, FR endosomes and transferrin receptor
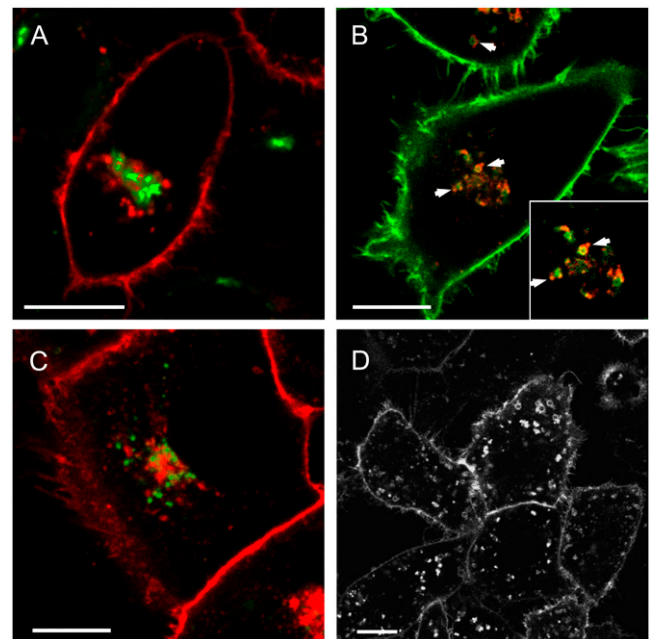

FIGURE 1 Intracellular itinerary of endocytosed FR. (A) FRs (pseudocolor red) were not delivered to the Golgi complex (pseudocolor green). Image was acquired 1 h after Golgi labeling by BODIPY-FL ceramide-BSA (5 μM). KB cells were labeled by 50 nM F-Rh for 30 min and incubated for 3 h to allow sufficient accumulation of FRs in the perinuclear area before Golgi labeling. (B) FRs (pseudocolor green) accumulated at the ERC, which is indicated by TfR (pseudocolor red) in KB cells. FRs and TfRs were associated but not completely colocalized as indicated by arrows. Image was acquired after 30 min labeling by F-BODIPY (50 nM) and TfR-Rh (0.5 μg/ml). (C) FRs (pseudocolor red) were not delivered to lysotracker positive compartment (pseudocolor green). Image was acquired 1.5 h after 30 min colabeling by 50 nM F-Rh and 100 nM Lysotracker Yellow HCK-123. (D) FR endosomes were not delivered to the ERC in cells where MTs have been disrupted with 10 μM colchicine for 2 h before F-Rh labeling. Image acquired 4 h after the labeling. Bar, 10 μm.

(TfR) endosomes trafficked to the same perinuclear area. However, careful analysis of the micrographs demonstrated that folate BODIPY-FL and transferrin rhodamine signals did not completely colocalize (Fig. 1 *B*), in agreement with electron microscopy observations that FR and TfR localize to different parts of irregular vesicles in KB cells (23). Furthermore, colocalization study of F-Rh and LysoTracker Yellow HCK-123 (*green*) revealed that FR endosomes are not delivered to lysotracker positive compartments such as late endosomes and lysosomes. These results indicate that endocytosed FRs are delivered to ERC but not the Golgi complex, late endosomes, or lysosomes in KB cells. Accumulation of FR endosomes in the ERC agrees with previous reports that recycling endosomes are enriched in raft components in CHO and Madin-Darby canine kidney cells (22,34,35).

In eukaryotic cells, movement of large compartments such as membranous organelles, secretory vesicles, and viral particles relies largely on active transport along MTs and MT-associated motor proteins (36). To evaluate the role of MTs in the transport of FR endosomes, we disrupted the MT network by treatment with colchicine and nocodazole. These two agents have been widely used for analyzing the role of MT in intracellular trafficking (29,37). In KB cells treated with colchicine or nocodazole, we observed a large number of FR endosomes in the cytoplasm, consistent with a previous observation that disruption of MT does not affect FR internalization (38). However, colchicine treatment impeded the usual accumulation of FR endosomes at the ERC, leading to their retention near the cell periphery (compare Fig. 1, *C* and *D*). These data demonstrate a critical role for the MT network in delivering FR endosomes to ERC in KB cells.

The MT-based movements of FR endosomes were directly visualized in HeLa cells stably transfected with GFP-tagged tubulin. Four hours after F-Rh labeling, FR endosomes were found concentrated in the MTOC (Fig. 2 *A*). Moreover, with the MT network stabilized by low-concentration PTX, we observed that most FR endosomes were associated with MTs (Fig. 2 *B*). An example of FR endosomes moving along MTs is displayed in Fig. 2, *C–E*, wherein the endosome moved 1.8 μm in 5.4 s, with an average speed of 0.33 μm/s (Movie 1, Supplementary Material). In some cases, the endosome was seen to switch from one MT to another after a pause at an MT junction (Movie 2, Supplementary Material). These results illustrate that MTs function as "highways" for the active transport of FR endosomes.

To identify motor proteins involved in the FR endosome motility, we employed inhibitory antibodies directed to the major MT motors (39,40). Cytoplasmic dynein is known to mediate the transport of various cargos to the minus end of MTs and retain the cargos there (36,41). To examine dynein's role in FR trafficking, anti-dynein antibodies were introduced into KB cells by microinjection. Importantly, anti-dynein antibody treatment did not inhibit internalization of FR. However, FR endosomes in the same treated cells
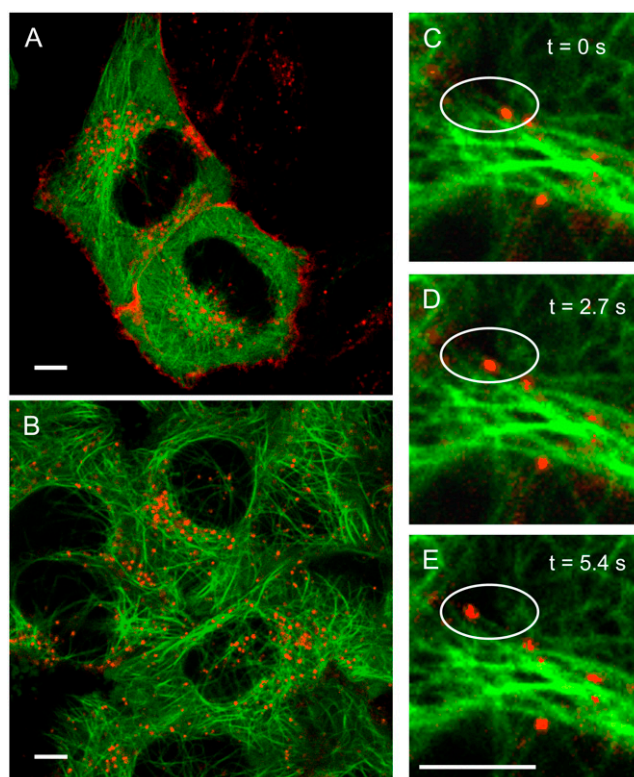

FIGURE 2 Movement of FR endosomes (pseudocolor *red*) along MTs (pseudocolor *green*) in HeLa cells stably transfected with GFP-tagged tubulin. The cells were incubated with F-Rh for 30 min at 37°C. Images were acquired 4 h later. (*A*) FR endosomes accumulated near MTOC. (*B*) FR endosomes were ubiquitously associated with MTs. To facilitate high-quality image acquisition, the dynamics of the MT network was suppressed by 30 min incubation with 60 nM PTX before imaging. (*C–E*) Sequential images of the same cell showing the movement of an FR endosome along a MT. The MT network inside the cell was stabilized by 60 nM PTX treatment. Bar, 5 μm.

became dispersed throughout the entire cytosol (Fig. 3 *A top right*, and Fig. 3 *B*), whereas they accumulated at ERC in cells not injected with anti-dynein antibody (Fig. 3 *A*). These results suggest that dynein is involved in delivering FR endosomes to the ERC.

To further define the role of dynein in regulating FR endosomal trafficking, FR endosomes were allowed to accumulate at the ERC (Fig. 3 *C*) before microinjection with anti-dynein antibody. As seen in Fig. 3 *D*, after 2 h additional incubation, the endosomes were again found scattered throughout the cytosol. These data suggest that FR endosomes are retained near the MTOC in part by dynein-mediated trafficking along MT toward their minus end.

In contrast to dynein, kinesin I has been shown to move vesicles toward the plus end of MT (36,42). To test whether this motor protein helps to recycle internalized FR to the cell surface, we introduced anti-kinesin I heavy chain antibodies into KB cells by microinjection and examined the distribution of FR endosomes after 30 min of F-Rh labeling at 37°C. In comparison with normal cells (Fig. 3 *E*), treatment with the
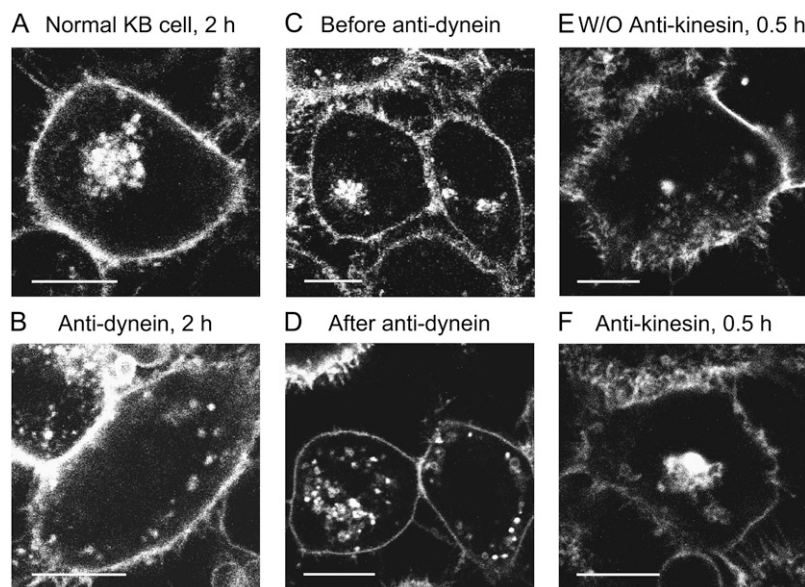
A Normal KB cell, 2 h
C Before anti-dynein
E W/O Anti-kinesin, 0.5 h
B Anti-dynein, 2 h
D After anti-dynein
F Anti-kinesin, 0.5 h

FIGURE 3 Roles of dynein and kinesin I in intracellular FR trafficking. (*A*) FR endosomes were delivered to the ERC in a normal KB cell. (*B*) FR endosomes were not delivered to the ERC in a KB cell with microinjection of anti-dynein antibody. For (*A*) and (*B*), cells were labeled with F-Rh after microinjection and then imaged 2 h later. (*C*) FR endosomes were delivered to the ERC in a normal KB cell. KB cells were labeled with F-Rh and incubated for 4 h before the antibody treatment. (*D*) Microinjection of dynein antibody scattered the FR endosomes previously localized at the ERC throughout the cytosol. The image was acquired 2 h after the injection. (*E*) Partially scattered distribution of FR endosomes in KB cells without anti-kinesin injection. (*F*) A more condensed accumulation of FR endosomes in the perinuclear area inside KB cells treated with kinesin I antibody by microinjection. For *E* and *F*, the images were acquired immediately after F-Rh labeling. For all images, F-Rh labeling was carried out for 30 min at 37°C, followed by three washes. Bar, 10 μm.

anti-kinesin I antibody led to more pronounced accumulation of FR endosomes in the perinuclear area (Fig. 3 *F*). These results suggest that kinesin I may be one of the kinesin motor proteins that mediate movement of FR endosomes away from the perinuclear region toward the MT plus end.

Single-particle tracking analysis of bidirectional motions of FR endosomes in single cells

To quantitatively characterize the motions of FR endosomes, we acquired time-lapse confocal fluorescence movies of KB cells labeled with F-Rh. A single frame from one movie is presented in Fig. 4 *A*. In this movie, we identified a total of 34 trajectories with durations between 10 and 30 s (Fig. 4 *B*). As shown in Fig. 4 *C*, the maximum instantaneous velocity (V_{max}) ranged from 0.25 to 1.5 μm/s. These values are comparable to previously reported maximum speeds (1.35–2.15 μm/s) of dynein-associated vesicles in *Dictyostelium discoideum* (43) and the in vitro speeds (1.4–2.8 μm/s) of dynein and kinesin-like motors in *Dictyostelium* extracts (44,45). Fig. 4 *D* shows the correlation between the maximal velocity (V_{max}) and the length of the trajectory of a representative selection of endosomes. It is clear that the endosomes with larger V_{max} values travel longer distances.

Intracellular bidirectional motions of particles have been reported (41). Using the SPT method, we identified two classes of bidirectional motions for individual FR endosomes. In an example of the first class (Fig. 5 *A*), an endosome with a V_{max} of 0.4 μm/s is seen to move a short distance, ~0.6 μm (Fig. 5 *B*), in a fashion that is characteristic of directed motion (Fig. 5 *D*). Using Eq. 1, the diffusion coefficient and the average velocity were obtained to be 0.00100 ($\pm$0.00003) μm^2/s and 0.0122 ($\pm$0.0003) μm/s, respectively. Importantly, the velocity is observed to change direction with 1 Hz frequency (Fig. 5 *C*). This result suggests

that dynein and kinesin can be associated with the same FR endosome, alternating their control of endosome movement with time. In the second case, shown in Fig. 5 *E*, the endosome exhibits bidirectional movement over a long distance along MTs (Movie 3, Supplementary Material), characterized by an oscillatory MSD curve (Fig. 5 *H*). Interestingly, we observed a gradual change in velocity during the direction

A Selected particles
B Trajectory duration
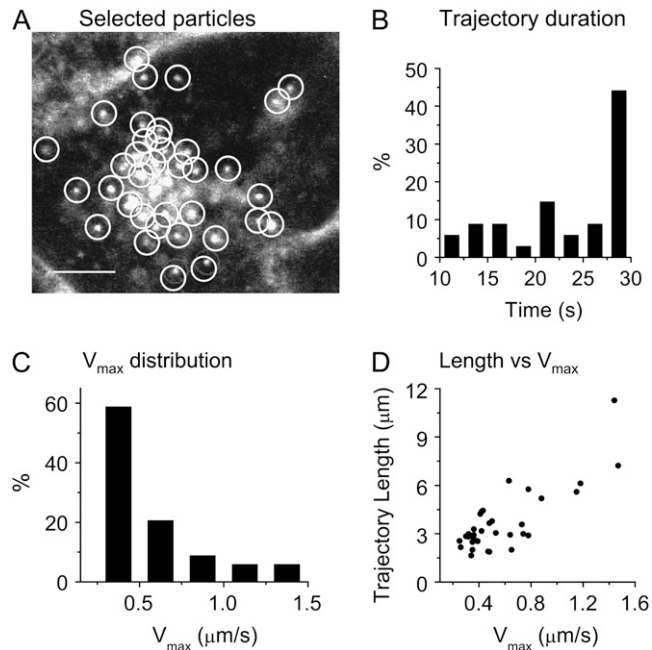C V_{max} distribution
D Length vs V_{max}

FIGURE 4 SPT analysis of FR endosomes in a single KB cell. (*A*) One frame from a video recording of FR endosome movement. For the endosomes marked with white circles, the trajectories and instantaneous velocities were measured by SPT. Bar, 5 μm. (*B*) Distribution of the trajectory durations. (*C*) Distribution of the trajectories' maximum instantaneous velocities. (*D*) Correlation between the trajectory length and the maximum instantaneous velocity. The 30-s movie was acquired at 4 h after 30 min labeling by F-Rh.
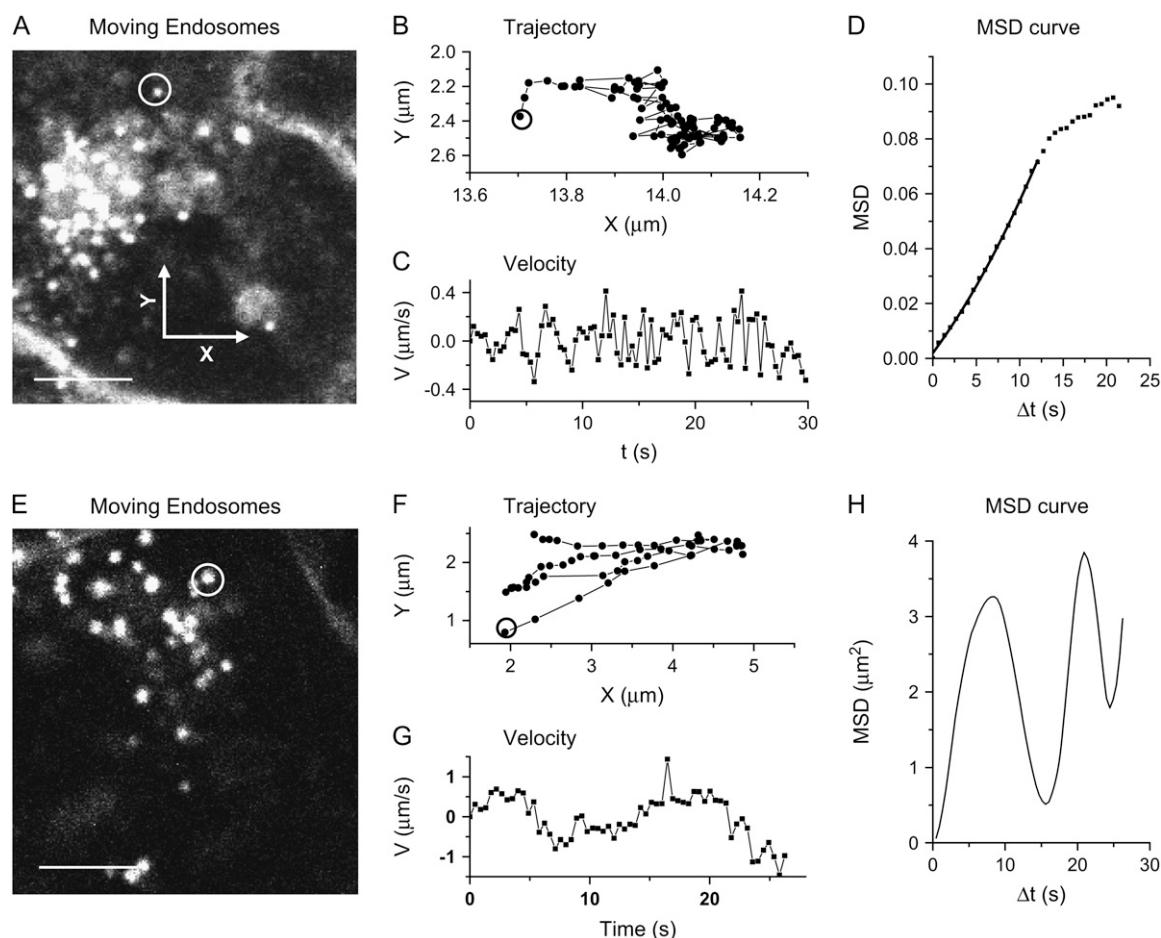
FIGURE 5 Bidirectional motions of FR endosomes (marked by *white ring*) inside KB cells. (*A*) An endosome that experienced bidirectional motion over a short distance. (*B–D*) The trajectory, instantaneous velocity, and MSD curve of the endosome marked in (*A*). For the lag time between 0 and 12.5 s, the MSD curve was well fitted with the active transport mode. The MSD dropped when the lag time exceeded 12.5 s due to the dominance of backward motion at the end of the trajectory. (*E*) An endosome that experienced bidirectional motion over a long distance. (*F–H*) The trajectory, instantaneous velocity, and MSD curve of the endosome marked in *E*.

switch (Fig. 5 *G*). Electron microscopy images (46) and stalling force measurements (47) have revealed that various motors participate in single-particle movements. Therefore, the gradual speed change could conceivably derive from a variation in the number and type of motors working on the endosome simultaneously.

In summary, the above analyses suggest that FR endosomes can move in both directions along the same MT. Dynein and kinesin I (KIF5) are involved in the delivery of FR endosomes toward the minus end and the plus end, respectively. Using the same methods, it should now be possible to quantitatively assay the impact of cellular cholesterol levels on the trafficking of FR endosomes, as described below.

Cholesterol depletion increases the motility of FR endosomes

We first tried lowering cellular cholesterol levels by metabolic depletion with compactin and achieved a reduction

of 30%, 60%, and 75% after 36, 60, and 84 h depletion, respectively (Fig. 6 *A*). Uptake of F-Rh by KB cells with different cholesterol contents is shown in Fig. 6 *B*. The plasma membrane was labeled by F-Rh in all cases. However, the intracellular F-Rh signal decreased as cholesterol was gradually depleted in the cell, consistent with the previously reported reduction of 5-methyltetrahydrofolate internalization in cholesterol-deprived MA104 cells (48). After 108 h of cholesterol depletion, complete inhibition of FR internalization was observed. Using [^{3}H]folic acid, the recycling rate was measured and $T_{1/2}$ was calculated to be 42 min for normal KB cells and 23 min for cells with 50% cholesterol depletion (Fig. 6, *C* and *D*). The higher recycling rate in cells containing less cholesterol was also observed in CHO cells stably transfected with FR (22).

To identify the mechanism underlying the observed change in the FR recycling rate upon cholesterol depletion, we quantitatively analyzed the trafficking of FR endosomes in normal and cholesterol-depleted KB cells. Through SPT
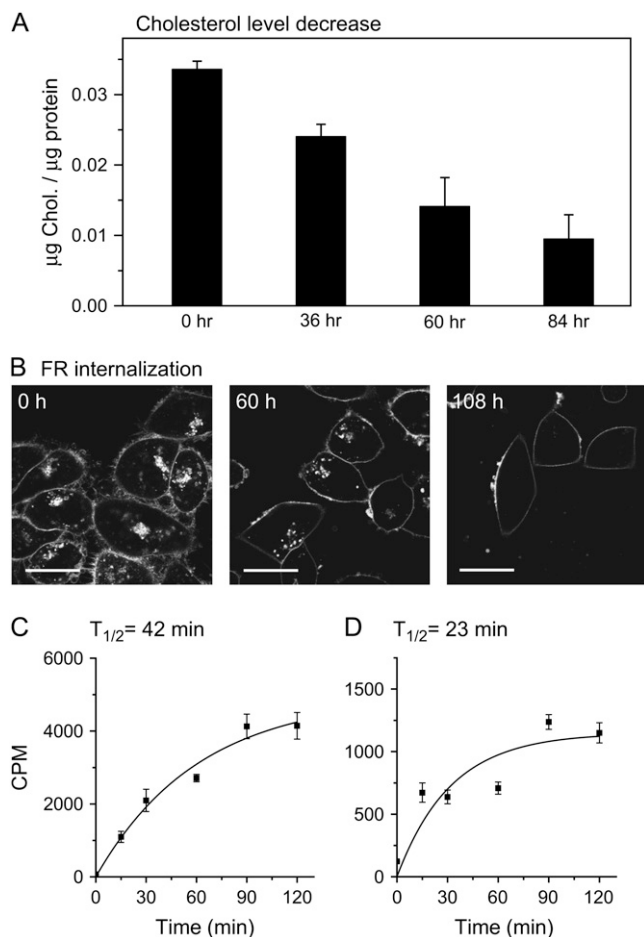
FIGURE 6 Impact of cholesterol depletion on FR internalization and recycling. (*A*) Cholesterol level in KB cells versus the depletion time. The cells were incubated in 5% lipoprotein-deficient serum supplemented with 250 μM mevalonate and 10 μM compactin for the indicated length of time. The cholesterol level, normalized by the protein level, was reduced by 30%, 60%, and 75% after depletion for 36, 60, and 84 h, respectively. (*B*) Internalization of FR in KB cells at different cholesterol levels. Images were acquired at 3 h after labeling. Bar, 20 μm. (*C* and *D*) [^{3}H]folic acid levels over time in normal and 50% cholesterol-deprived KB cells. The recycling curves were fitted with an exponential model (see Materials and Methods), generating $T_{1/2}$ = 42 min and 23 min for normal and cholesterol-depleted KB cells, respectively.
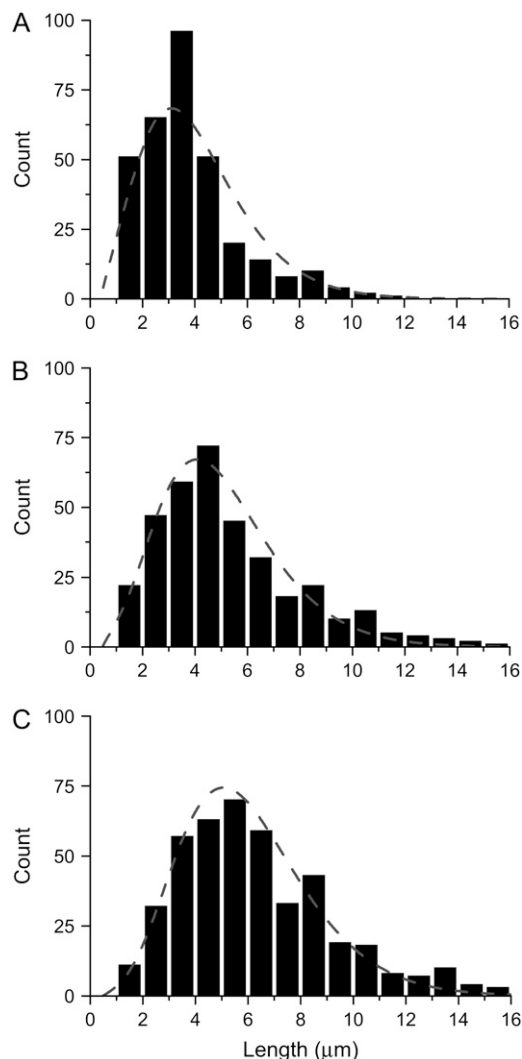

FIGURE 7 Distribution of trajectory lengths in normal and cholesterol-depleted KB cells. Movies with 30 s duration were acquired between 3 and 4 h after 30 min labeling by F-Rh. The dashed lines represent least-squares fitting by Poisson probability mass function, $f(k;\lambda) = e^{-\lambda}\lambda^k/k!$, where λ represents the average length of trajectory. (*A*) Length distribution of 322 trajectories obtained from 10 normal KB cells, $\lambda = 2.95$ μm. (*B*) Length distribution of 356 trajectories obtained from 10 KB cells with metabolic depletion of cholesterol by compactin, $\lambda = 4.31$ μm. (*C*) Length distribution of 438 trajectories from 10 KB cells with acute membrane cholesterol depletion by MβCD, $\lambda = 4.69$ μm.

analysis of 30-s movies, we obtained a total of 322 FR endosome trajectories in 10 normal KB cells and 356 trajectories in 10 KB cells depleted to 50% of their normal cholesterol. A remarkable increase in trajectory lengths was observed for the cholesterol-depleted cells (Fig. 7, *A* and *B*). Because the trajectory length is strongly correlated with V_{max} (Fig. 4 *D*), our result indicates an enhancement of FR endosome motility caused by lowering cellular cholesterol. Importantly, this conclusion could be confirmed using an independent method of cholesterol depletion, where cholesterol was extracted directly from the plasma membrane using MβCD extraction. As seen in Fig. 7 *C*, a similar change of FR endosome motility was obtained from the analysis of 438

trajectories from 10 KB cells. Taken together, these results demonstrate that endosomal cholesterol regulates FR endosome motility.

To quantify the increase of motility, we fitted the distributions of trajectory lengths using the Poisson possibility mass function, $f(k;\lambda) = e^{-\lambda}\lambda^k/k!$, where λ is the mean as well as the variance and k is a nonnegative integer. By least-squares fitting, the maximum likelihood estimator of λ (the expected length of the trajectory) was found to be 2.95 μm for normal KB cells, 4.31 μm for KB cells with metabolic cholesterol depletion, and 4.69 μm for KB cells with acute

cholesterol extraction. This result quantitatively demonstrates the enhanced motility of FR endosomes in cholesterol-depleted KB cells.

We further correlated the increased motility with motor activities. Because FR endosomes exhibited bidirectional movement characterized by frequent switches between plus and minus speeds, we carried out a statistical analysis of the distribution of instantaneous velocities measured in 10 normal cells and 10 cells metabolically depleted of cholesterol. The data (Fig. S1, Supplementary Material) show that V_{max} toward the MT plus end is increased in cells with lowered cholesterol, whereas V_{max} toward the MT minus end is little affected. SPT analysis of FR endosomes in a cholesterol-deprived cell is shown in Fig. S1 C, where two endosomes travel toward the MT minus end and the plus end, respectively. The instantaneous velocities to the MT minus end were seen to be similar to those in normal KB cells, whereas the FR endosome moving to the MT plus end had a V_{max} of 1.80 μm/s, which is 20% larger than that in normal KB cells. These results suggest that the increased motility is correlated with a reduced activity of dynein and an enhanced activity of kinesin associated with FR endosomes.

Cholesterol regulates intracellular FR transport via Rab7 and Rab4 proteins

We hypothesized that the enhanced motility of FR endosomes in cholesterol-depleted cells was not a direct conse-

quence of a change in physical properties of the endosomal membranes, but rather might derive from a modulation of motor protein association with the cholesterol-depleted endosomes, perhaps mediated by Rab proteins. It is well established that a large number of Rab proteins and their effectors regulate endocytic trafficking (49). In the Rab protein family, for example, activities of Rab4, Rab7, and Rab9 are known to be affected by endosome cholesterol levels (50–52). However, because Rab9 has been previously shown to control transport between late endosomes and the trans-Golgi network (53) and FR endosomes were not delivered to the Golgi complex in either KB cells (Fig. 1 A) or CHO cells (22,54), we excluded Rab9 from our study.

To begin to characterize the possible roles of Rab7 and Rab4 in mediating the above cholesterol effect, we transfected KB cells with either Rab7-GFP or Rab4-GFP and carried out colocalization studies of Rab proteins and FR endosomes. In KB cells transfected with Rab7-GFP, green rings (Rab7) displaying red (F-Rh) fluorescent interiors were observed at 30 min and 2 h after the F-Rh labeling (Fig. 8 A). On the other hand, in similar studies with Rab4-GFP-transfected cells, no overlap between Rab4-GFP (*green*) and F-Rh (*red*) fluorescence was seen (Fig. 8 C). These data suggest that Rab7 is recruited by FR endosomes soon after internalization, whereas Rab4 is largely excluded from the same endosomes.

To confirm the involvement of Rab7 in the MT-dependent motion of FR endosomes, we transfected KB cells with a
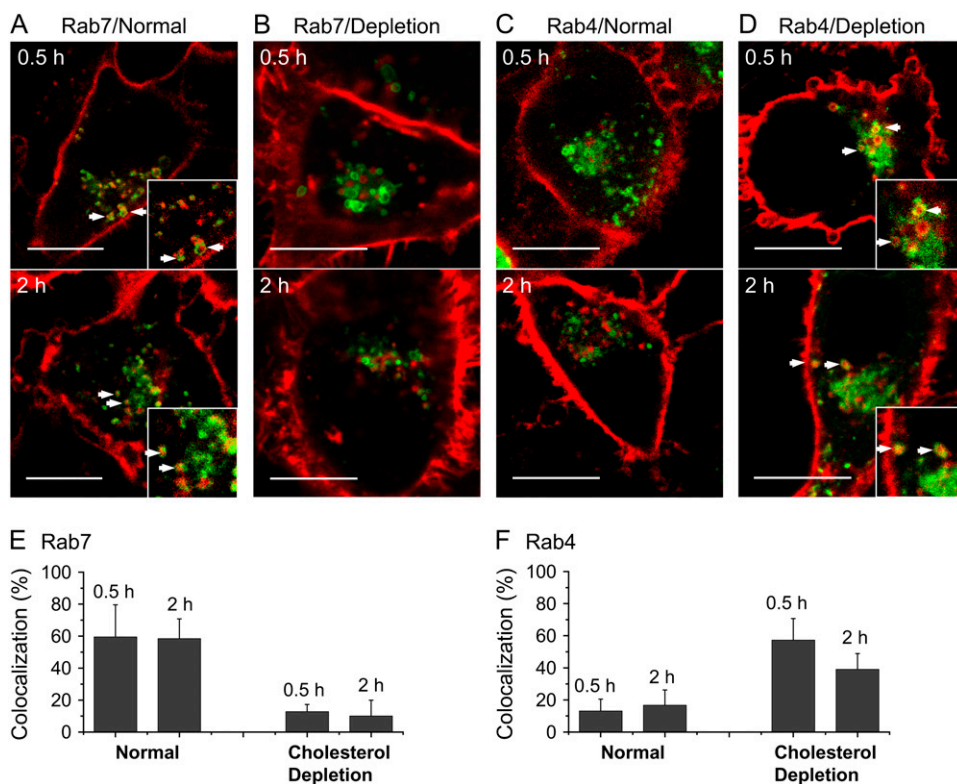

FIGURE 8 Cholesterol-dependent association of Rab7 and Rab4 with FR endosomes. (*A*) Rab7 was efficiently recruited by FR endosomes in normal KB cells. Arrows indicate the colocalization of Rab7 and FR endosomes. (*B*) The colocalization of FR endosomes with Rab7 protein was decreased in metabolic cholesterol-depleted KB cells. (*C*) Rab4 is not colocalized with FR endosomes in normal KB cells. (*D*) The colocalization of FR endosomes with Rab4 protein was observed as arrows indicate in cholesterol-depleted KB cells. Bar, 10 μm. (*E*) Percentage of FR endosomes colocalized with Rab7-GFP in normal and cholesterol-depleted KB cells. (*F*) Percentage of FR endosomes colocalized with Rab4-GFP in normal and cholesterol-depleted KB cells. Only those endosomes with complete overlap of red and green signals or with a red core in a green ring were counted as colocalization. The significance of the difference was analyzed by t-test, with a result of $p < 0.001$. For each data set, ~100 endosomes chosen from ~9 cells were analyzed.

dominant-negative version of Rab7, GFP-Rab7N125I. As expected, F-Rh colocalized with GFP-Rab7N125I on FR endosomes, suggesting that dominant negative Rab7 had successfully substituted for endogenous Rab7. Moreover, the FR endosomes were significantly scattered throughout the cytoplasm in the presence of GFP-Rab7N125I (Fig. S2, Supplementary Material), implying that the trafficking function of endogenous Rab7 was successfully inhibited. Because the Rab4 proteins are only marginally associated with FR endosomes, overexpression of dominant negative Rab4 did not result in any obvious alteration of FR endocytosis (data not shown).

Importantly, we observed that cholesterol depletion alters the above pattern of association of Rab7 and Rab4 with FR endosomes. In KB cells depleted to 50% of their normal cholesterol (metabolic method), Rab7-GFP and F-Rh were found largely separated (Fig. 8 *B*), indicating significantly decreased Rab7 association with FR endosomal membranes. Meanwhile, green ring structures (Rab4) with red F-Rh interiors were observed at 30 min and 2 h (Fig. 8 *D*), indicating an increased recruitment of Rab4 to the FR endosomal membrane.

To quantify the shift in the colocalization of FR endosomes from Rab7 to Rab4, we calculated a recruitment percentage, defined as the number of endosomes which showed complete overlap of F-Rh (*red*) and GFP-Rab protein (*green*) divided by the total number of endosomes. For each condition, ~100 endosomes from ~9 cells were analyzed with the same standard. The results demonstrate that cholesterol depletion decreases association of Rab7 with FR endosomes 4.7-fold by 0.5 h and 5.8-fold by 2 h after F-Rh internalization. (Fig. 8 *E*). In contrast, the cholesterol depletion increases interaction of Rab4 with FR endosomes by 4.4- and 2.3-fold at 0.5 and 2 h, respectively (Fig. 8 *F*).

Because Rab7 was known as an adaptor of dynein motor protein (51,55), we further studied the association of dynein with FR endosomes under different cholesterol levels by immunofluorescence. The dynactin projecting arm p150^{Glued} was shown to be required for dynein motor recruitment to endosomes (55). By using anti-p150^{Glued}, we found that p150^{Glued} (*green*) was accumulated and significantly colocalized with FR endosomes (*red*) in the ERC area in normal KB cells (Fig. 9 *A*), indicating that FR endosomes efficiently recruited dynein motor proteins. However, such accumulation of p150^{Glued} (*green*) was not observed in cholesterol-depleted KB cells (Fig. 9 *B*), suggesting that cholesterol depletion impairs the recruitment of dynein by FR endosomes. This result is consistent with our Rab7 studies shown in Fig. 8.

DISCUSSION

Intracellular active transport relies on the function of different motor proteins that transport cargo along cytoskeleton tracks. Cells may regulate this transport in a variety of ways, including via changes in phosphorylation of motor-associated proteins catalyzed by protein kinase A, protein kinase C, and protein phosphatase 2A (56,57). The observed cholesterol regulation of FR endosome motility in this work suggests that endosome trafficking along MTs can be alternatively regulated by modulating the coordination between motor proteins and Rab GTPases via changes in endosomal cholesterol level.

Rab GTPases form one group of potential receptors for motor proteins (58). Along with a wide variety of effectors, Rab proteins directly or indirectly interact with motor proteins or their subunits and link the motors to vesicle membranes. For example, Rab7 proteins were shown to retain
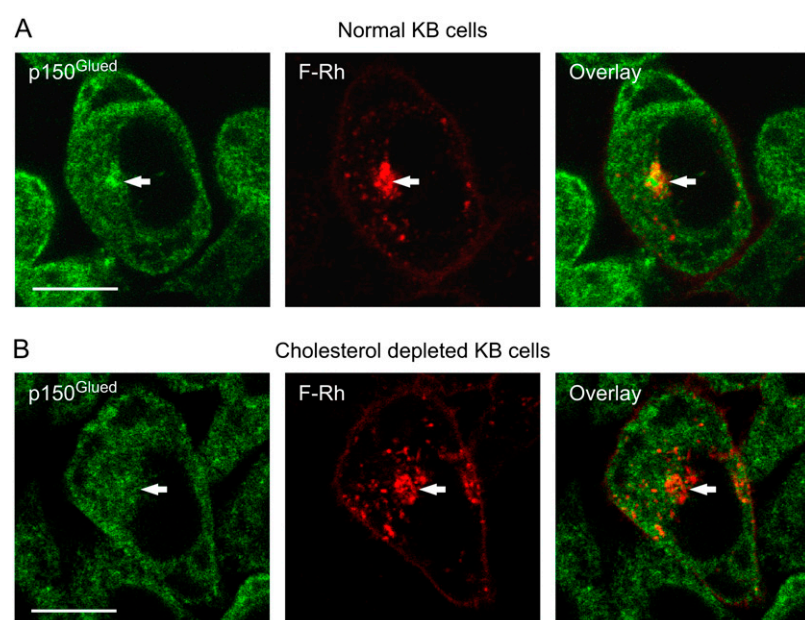

FIGURE 9 Cholesterol-dependent association of p150^{Glued} with FR endosomes. Anti-p150^{Glued} was visualized with Cy2 secondary antibody conjugates (*green*). FR endosomes were labeled by F-Rh (*red*). (*A*) p150^{Glued} was efficiently recruited by FR endosomes and accumulated in the ERC area in normal KB cells as the arrow indicates. (*B*) Accumulation of p150^{Glued} in the ERC area was not observed in cholesterol-depleted KB cells, whereas FR endosomes were still found in the ERC area as the arrow indicates. Bar, 10 μm.

dynein activity but not kinesin activity; Rab4 has been established as an adaptor of KIF3 and KIFC2 and thereby assists the endosome to recruit motor proteins for outward as well as inward transport (59,60); Rab11 was considered to be a linker between *osk* mRNA and kinesin I (61). Further, such interaction may serve to recruit and release the motors from the vesicles in a manner controlled by the nucleotide state of the GTPase switch (62). Meanwhile, Rab GTPases as lipid-modulated proteins are localized to the cytoplasmic surface of distinct compartments inside the cell (63). They are ubiquitous components of membrane-bound vesicle trafficking machines, with different Rab proteins regulating traffic between different intracellular compartments (64). Although the specific localization of Rab proteins is not well understood, previous studies have shown that activities of Rab4, Rab7, and Rab9 proteins are regulated by cholesterol (50–52).

In this work, we showed that FR endosomes are delivered to ERC (Fig. 1) and retained around MTOC with a relatively slow recycling rate (Fig. 6). These properties can be well understood in terms of the functions of Rab proteins. In normal KB cells, it was observed that FR endosomes would efficiently recruit Rab7 rapidly after endocytosis (Fig. 8 *A*). Because Rab7 proteins have been shown to promote late endosome retention of dynein activity (51), it is conceivable that they help FR endosomes retain dynein as well, which facilitates delivery of FRs to the recycling compartment near the MTOC. In the recycling compartment, the retention promoted by dynein competes with the recycling by kinesins, contributing to the slower recycling of GPI-anchored proteins than TfR (22).

It is known that endocytic recycling occurs by a fast and a slow route (4,65). Rab4 and Rab11, which exhibit a distinct but partially overlapping distribution in cells (66), are involved in these two routes. Rab4 is physically associated with motor protein KIF3 (59) and mainly involved in fast recycling from early endosomes (67), whereas Rab11 mainly facilitates slow recycling from the recycling endosomes (68). Endocytosed FRs were not found colocalized with Rab4 in either KB cells (Fig. 8 *C*) or FR-transfected CHO cells (21), possibly because of a higher cholesterol level in the FR compartments. This result indicates that FR endosomes are not able to effectively recruit Rab4-associated kinesin motors, possibly KIF3. Consequently, FRs cannot be recycled to the cell surface via the fast recycling route. Instead, our data suggest that FRs may be recycled through Rab11 (Fig. S3, Supplementary Material). This mechanism partially accounts for the slower recycling rate of FR than TfR (22), because it was reported that 90% of the TfR was associated with Rab4 in early endosomes (66) and Rab4 overexpression increases the early recycling rates of TfR (69).

An important observation of this work is that cholesterol depletion increases the motility of FR endosomes. We attribute the observed cholesterol-dependent motility to the regulation of affinities of Rab4 and Rab7 for FR endosomes through dynein and kinesin motor proteins. It is notable that myosin V, an actin-based motor, was shown to behave as a drag that can retard the translation of organelles along MTs in dendritic extensions of melanocytes (70). However, the KB cells used in our study do not have such ''dendritic extensions'' where the F-actin could effectively interact with
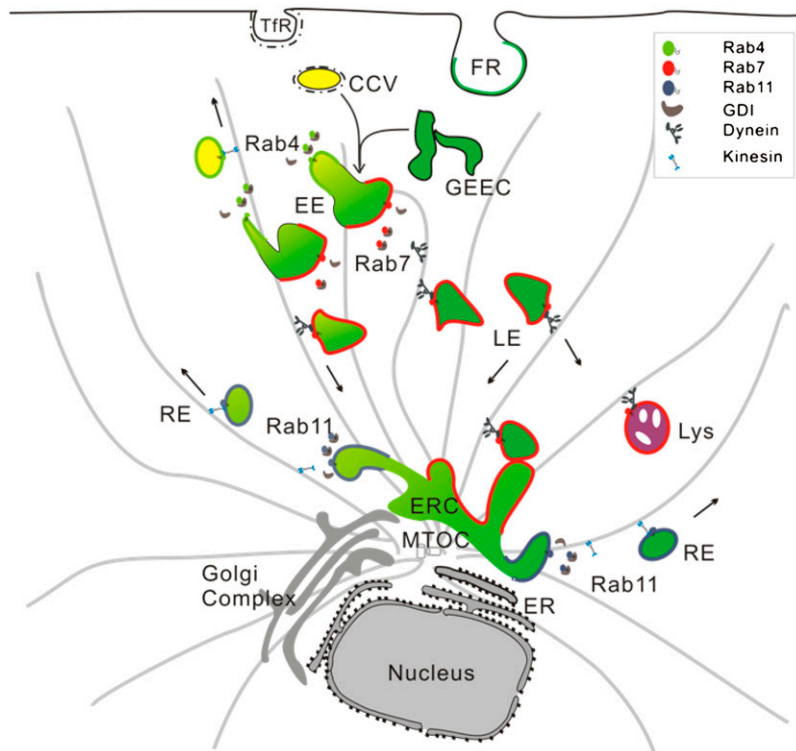

FIGURE 10 Diagram illustrating the roles of Rab proteins in trafficking of FR and TfR endosomes. After internalization, FR enters the GPI-anchored protein-enriched early endosomal compartment (*GEEC*) and TfR enters the clathrin-coated vesicle (*CCV*). The internalized TfRs and FRs then merge into the early endosomal system. The FR compartments which recruit Rab7 effectively are delivered to the ERC by dynein, whereas the TfR compartments are partially recycled back by Rab4. The enhanced dynein activity retains FRs at the ERC. Meanwhile, part of FRs and TfRs can be recycled to the cell surface through Rab11 and associated motor proteins. In parallel with the endocytic recycling, a portion of the early endosomes can also mature into late endosome (*LE*) and lysosomes (*Lys*).

the MT-based transport. Therefore, we believe that myosin V does not play a significant role in the MT-based motions of FR-endosomes.

As shown in Fig. 8 *B*, cholesterol depletion downregulates Rab7 recruitment by FR endosomes, which is thought to impair the dynein association. Indeed, we found that cholesterol depletion reduces the accumulation of p150$^{\text{Glued}}$ in the ERC area (Fig. 9). In addition to Rab7, Rab4 is also thought to be responsible for increased endosome motility and FR recycling in cholesterol-depleted cells where an extensive coating of Rab4-GFP on the FR endosomes was observed (Fig. 8 *D*). Because Rab4 was shown to be physically associated with KIF3 (59), it is possible that cholesterol depletion increases the association of Rab4 proteins and thus KIF3 with FR endosomes. Therefore, the decreased dynein activity and increased KIF3 activity should enhance the motility of FR endosomes, as observed in Fig. 7, *A–C*. This increased motility was shown to correlate with enhanced movement toward the MT plus end (Fig. S1), which facilitates the escape of endosomes from the MTOC area. These changes would be expected to contribute to the faster recycling of FRs in cholesterol-deprived KB cells (Fig. 6 *D*).

Similar cholesterol regulation of intracellular transport has also been observed in other systems. Gruenberg and co-workers reported that cholesterol regulates the motility of late endosomes (51). They found that elevating the cholesterol level increases the amounts of Rab7, leading to a paralysis of late endocytic compartments due to the retention of dynein activity and loss of kinesin activity. In this work, we explored the effect of lowering the cholesterol level on intracellular trafficking of FR endosomes. We showed that cholesterol depletion increases the motility of endosomes through Rab proteins and associated motor proteins. Furthermore, we found both Rab7 and Rab4 contribute to this process.

A diagram summarizing the roles of Rab proteins in the trafficking of FR endosomes is shown in Fig. 10. TfR, for which the role of Rab proteins has been well studied (66,69), was added as a reference. After internalization, FR enters the GPI-anchored protein-enriched early endosomal compartment, whereas TfR independently enters via a clathrin-coated vesicle. The internalized TfRs and FRs then merge into the early endosomal system. The FR compartment which recruits Rab7 effectively is delivered to the ERC by dynein, whereas the TfR compartment is partially recycled back by Rab4 on its way to the ERC. The enhanced dynein activity retains FRs at the ERC. Meanwhile, part of the FR can be recycled to the cell surface through Rab11 and associated motor proteins.

In summary, the motility of FR-containing endosomes in normal and cholesterol-deprived KB cells has been characterized by the SPT method. Cholesterol depletion increases endosome motility toward the MT plus end by downregulating the FR endosome's association with Rab7 GTPase and increasing its association with Rab4 GTPase. The increased Rab4 recruitment could partially switch the

recycling of FRs to the fast recycling route mediated by Rab4. These results show that cholesterol is a possible modulator of intracellular membrane trafficking. In general, our study suggests an intriguing role for lipids in the intracellular delivery of membrane-bound compartments.

SUPPLEMENTARY MATERIAL

To view all of the supplemental files associated with this article, visit www.biophysj.org.

REFERENCES

1. Mukherjee, S., R. N. Ghosh, and F. R. Maxfield. 1997. Endocytosis. *Physiol. Rev.* 77:759–803.

2. Helms, J. B., and C. Zurzolo. 2004. Lipids as targeting signals: lipid rafts and intracellular trafficking. *Traffic.* 5:247–254.

3. Maxfield, F. R., and D. Wustner. 2002. Intracellular cholesterol transport. *J. Clin. Invest.* 110:891–898.

4. Gruenberg, J. 2001. The endocytic pathway: a mosaic of domains. *Nat. Rev. Mol. Cell Biol.* 2:721–730.

5. Chatterjee, S., and S. Mayor. 2001. The GPI-anchor and protein sorting. *Cell. Mol. Life Sci.* 58:1969–1987.

6. Fivaz, M., F. Vilbois, S. Thurnheer, C. Pasquali, L. Abrami, P. E. Bickel, R. G. Parton, and F. G. van der Goot. 2002. Differential sorting and fate of endocytosed GPI-anchored proteins. *EMBO J.* 21:3989–4000.

7. Abrami, L., S. Liu, P. Cosson, S. H. Leppla, and F. G. van der Goot. 2003. Anthrax toxin triggers endocytosis of its receptor via a lipid raft-mediated clathrin-dependent process. *J. Cell Biol.* 160:321–328.

8. Zhang, M., N. K. Dwyer, D. C. Love, A. Cooney, M. Comly, E. Neufeld, P. G. Pentchev, E. J. Blanchette-Mackie, and J. A. Hanover. 2001. Cessation of rapid late endosomal tubulovesicular trafficking in Niemann-Pick type C1 disease. *Proc. Natl. Acad. Sci. USA.* 98:4466–4471.

9. Karten, B. A., D. E. Vance, R. B. Campenot, and J. E. Vance. 2003. Trafficking of cholesterol from cell bodies to distal axons in Niemann Pick C1-deficient neurons. *J. Biol. Chem.* 278:4168–4175.

10. Pagano, R. E. 2003. Endocytic trafficking of glycosphingolipids in sphingolipid storage diseases. *Philos. Trans. R. Soc. Lond. B Biol. Sci.* 358:885–891.

11. Kamen, B. A., M. T. Wang, A. J. Streckfuss, X. Peryea, and R. G. Anderson. 1988. Delivery of folates to the cytoplasm of MA104 cells is mediated by a surface membrane receptor that recycles. *J. Biol. Chem.* 263:13602–13609.

12. Kamen, B. A., and A. K. Smith. 2004. A review of folate receptor alpha cycling and 5-methyltetrahydrofolate accumulation with an emphasis on cell models in vitro. *Adv. Drug Deliv. Rev.* 56:1085–1097.

13. Mayor, S., and H. Riezman. 2004. Sorting GPI-anchored proteins. *Nat. Rev. Mol. Cell Biol.* 5:110–120.

14. Varma, R., and S. Mayor. 1998. GPI-anchored proteins are organized in submicron domains at the cell surface. *Nature.* 394:798–801.

15. Ikonen, E. 2001. Roles of lipid rafts in membrane transport. *Curr. Opin. Cell Biol.* 13:470–477.

16. Rothberg, K. G., Y. S. Ying, J. F. Kolhouse, B. A. Kamen, and R. G. Anderson. 1990. The glycophospholipid-linked folate receptor internalizes folate without entering the clathrin-coated pit endocytic pathway. *J. Cell Biol.* 110:637–649.

17. Anderson, R. G., B. A. Kamen, K. G. Rothberg, and S. W. Lacey. 1992. Potocytosis: sequestration and transport of small molecules by caveolae. *Science.* 255:410–411.

18. Mayor, S., K. G. Rothberg, and F. R. Maxfield. 1994. Sequestration of GPI-anchored proteins in caveolae triggered by cross-linking. *Science.* 264:1948–1951.

19. Wu, M., J. Fan, W. Gunning, and M. Ratnam. 1997. Clustering of GPI-anchored folate receptor independent of both cross-linking and association with caveolin. *J. Membr. Biol.* 159:137–147.

20. Ritter, T. E., O. Fajardo, H. Matsue, R. G. W. Anderson, and S. W. Lacey. 1995. Folate receptors targeted to clathrin-coated pits cannot regulate vitamin uptake. *Proc. Natl. Acad. Sci. USA.* 92:3824–3828.

21. Sabharanjak, S., P. Sharma, R. G. Parton, and S. Mayor. 2002. GPI-anchored proteins are delivered to recycling endosomes via a distinct cdc42-regulated, clathrin-independent pinocytic pathway. *Dev. Cell.* 2:411–423.

22. Mayor, S., S. Sabharanjak, and F. R. Maxfield. 1998. Cholesterol-dependent retention of GPI-anchored proteins in endosomes. *EMBO J.* 17:4626–4638.

23. Turek, J. J., C. P. Leamon, and P. S. Low. 1993. Endocytosis of folate-protein conjugates: ultrastructural localization in KB cells. *J. Cell Sci.* 106:423–430.

24. Yang, J., H. Chen, I. R. Vlahov, J.-X. Cheng, and P. S. Low. 2006. Evaluation of disulfide reduction during receptor-mediated endocytosis by using FRET imaging. *Proc. Natl. Acad. Sci. USA.* 103:13872–13877.

25. Paulos, C. M., J. A. Reddy, C. P. Leamon, M. J. Turk, and P. S. Low. 2004. Ligand binding and kinetics of folate receptor recycling in vivo: impact on receptor-mediated drug delivery. *Mol. Pharmacol.* 66:1406–1414.

26. Yang, J., H. Chen, I. R. Vlahov, J.-X. Cheng, and P. S. Low. 2007. Characterization of the pH folate receptor-containing endosomes and the rate of hydrolysis of internalized acid-labile folate-drug conjugates. *J. Pharmacol. Exp. Ther.* 321:462–468.

27. Chatterjee, S., E. R. Smith, K. Hanada, V. L. Stevens, and S. Mayor. 2001. GPI anchoring leads to sphingolipid-dependent retention of endocytosed proteins in the recycling endosomal compartment. *EMBO J.* 20:1583–1592.

28. Saxton, M. J., and K. Jacobson. 1997. Single-particle tracking: applications to membrane dynamics. *Annu. Rev. Biophys. Biomol. Struct.* 26:373–399.

29. Lakadamyali, M., M. J. Rust, H. P. Babcock, and X. Zhuang. 2003. Visualizing infection of individual influenza viruses. *Proc. Natl. Acad. Sci. USA.* 100:9280–9285.

30. Yvon, A.-M. C., P. Wadsworth, and M. A. Jordan. 1999. Taxol suppresses dynamics of individual microtubules in living human tumor cells. *Mol. Biol. Cell.* 10:947–959.

31. Crocker, J. C., and D. G. Grier. 1996. Methods of digital video microscopy for colloidal studies. *J. Colloid Interface Sci.* 179:298–310.

32. Johnson, L. S., K. W. Dunn, B. Pytowski, and T. E. McGraw. 1993. Endosome acidification and receptor trafficking: bafilomycin A1 slows receptor externalization by a mechanism involving the receptor's internalization motif. *Mol. Biol. Cell.* 4:1251–1266.

33. Lin, S. X., G. G. Gundersen, and F. R. Maxfield. 2002. Export from pericentriolar endocytic recycling compartment to cell surface depends on stable, detyrosinated (Glu) microtubules and kinesin. *Mol. Biol. Cell.* 13:96–109.

34. Mukherjee, S., X. Zha, I. Tabas, and F. R. Maxfield. 1998. Cholesterol distribution in living cells: fluorescence imaging using dehydroergosterol as a fluorescent cholesterol analog. *Biophys. J.* 75:1915–1925.

35. Gagescu, R., N. Demaurex, R. G. Parton, W. Hunziker, L. A. Huber, and J. Gruenberg. 2000. The recycling endosome of Madin-Darby canine kidney cells is a mildly acidic compartment rich in raft components. *Mol. Biol. Cell.* 11:2775–2791.

36. Murray, J. W., and A. W. Wolkoff. 2003. Roles of the cytoskeleton and motor proteins in endocytic sorting. *Adv. Drug Deliv. Rev.* 55:1385–1403.

37. Fletcher, L. M., G. I. Welsh, P. B. Oatey, and J. M. Tavaré. 2000. Role for the microtubule cytoskeleton in GLUT4 vesicle trafficking and in the regulation of insulin-stimulated glucose uptake. *Biochem. J.* 352:267–276.

38. Lewis, C. M., A. K. Smith, and B. A. Kamen. 1998. Receptor-mediated folate uptake is positively regulated by disruption of the actin cytoskeleton. *Cancer Res.* 58:2952–2956.

39. Lippincott-Schwartz, J., N. B. Cole, A. Marotta, P. A. Conrad, and G. S. Bloom. 1995. Kinesin is the motor for microtubule-mediated Golgi-to-ER membrane traffic. *J. Cell Biol.* 128:293–306.

40. Ichikawa, T., M. Yamada, D. Homma, R. J. Cherry, I. E. G. Morrison, and S. Kawato. 2000. Digital fluorescence imaging of trafficking of endosomes containing low-density lipoprotein in brain astroglial cells. *Biochem. Biophys. Res. Commun.* 269:25–30.

41. Hirokawa, N. 1998. Kinesin and dynein superfamily proteins and the mechanism of organelle transport. *Science.* 279:519–526.

42. Hirokawa, N. 1996. Organelle transport along microtubules—the role of KIFs. *Trends Cell Biol.* 6:135–141.

43. Ma, S., and R. L. Chisholm. 2002. Cytoplasmic dynein-associated structures move bidirectionally in vivo. *J. Cell Sci.* 115:1453–1460.

44. McCaffrey, G., and R. D. Vale. 1989. Identification of a kinesin-like microtubule-based motor protein in Dictyostelium discoideum. *EMBO J.* 8:3229–3234.

45. Pollock, N., M. P. Koonce, E. L. de Hostos, and R. D. Vale. 1998. In vitro microtubule-based organelle transport in wild-type Dictyostelium and cells overexpressing a truncated dynein heavy chain. *Cell Motil. Cytoskeleton.* 40:304–314.

46. Habermann, A., T. A. Schroer, G. Griffiths, and J. K. Burkhardt. 2001. Immunolocalization of cytoplasmic dynein and dynactin subunits in cultured macrophages: enrichment on early endocytic organelles. *J. Cell Sci.* 114:229–240.

47. Welte, M. A., S. P. Gross, M. Postner, S. M. Block, and E. F. Wieschaus. 1998. Developmental regulation of vesicle transport in Drosophila embryos: forces and kinetics. *Cell.* 92:547–557.

48. Chang, W. J., K. G. Rothberg, B. A. Kamen, and R. G. Anderson. 1992. Lowering the cholesterol content of MA104 cells inhibits receptor-mediated transport of folate. *J. Cell Biol.* 118:63–69.

49. Novick, P., and M. Zerial. 1997. The diversity of Rab proteins in vesicle transport. *Curr. Opin. Cell Biol.* 9:496–504.

50. Choudhury, A., M. Dominguez, V. Puri, D. K. Sharma, K. Narita, C. L. Wheatley, D. L. Marks, and R. E. Pagano. 2002. Rab proteins mediate Golgi transport of caveola-internalized glycosphingolipids and correct lipid trafficking in Niemann-Pick C cells. *J. Clin. Invest.* 109:1541–1550.

51. Lebrand, C., M. Corti, H. Goodson, P. Cosson, V. Cavalli, N. Mayran, J. Fauré, and J. Gruenberg. 2002. Late endosome motility depends on lipids via the small GTPase Rab7. *EMBO J.* 21:1289–1300.

52. Choudhury, A., D. K. Sharma, D. L. Marks, and R. E. Pagano. 2004. Elevated endosomal cholesterol levels in Niemann-Pick cells inhibit Rab4 and perturb membrane recycling. *Mol. Biol. Cell.* 15:4500–4511.

53. Lombardi, D., T. Soldati, M. A. Riederer, Y. Goda, M. Zerial, and S. R. Pfeffer. 1993. Rab9 functions in transport between late endosomes and the trans Golgi network. *EMBO J.* 12:677–682.

54. Nichols, B. J., A. K. Kenworthy, R. S. Polishchuk, R. Lodge, T. H. Roberts, K. Hirschberg, R. D. Phair, and J. Lippincott-Schwartz. 2001. Rapid cycling of lipid raft markers between the cell surface and Golgi complex. *J. Cell Biol.* 153:529–542.

55. Johansson, M., N. Rocha, W. Zwart, I. Jordens, L. Janssen, C. Kuijl, V. M. Olkkonen, and J. Neefjes. 2007. Activation of endosomal dynein motors by stepwise assembly of Rab7-RILP-p150Glued, ORP1L, and the receptor βIII spectrin. *J. Cell Biol.* 176:459–471.

56. McIlvain, J. M. Jr., J. K. Burkhardt, S. Hamm-Alvarez, Y. Argon, and M. P. Sheetz. 1994. Regulation of kinesin activity by phosphorylation of kinesin-associated proteins. *J. Biol. Chem.* 269:19176–19182.

57. Reilein, A. R., I. S. Tint, N. I. Peunova, G. N. Enikolopov, and V. I. Gelfand. 1998. Regulation of organelle movement in melanophores by protein kinase A (PKA), protein kinase C (PKC), and protein phosphatase 2A (PP2A). *J. Cell Biol.* 142:803–813.

58. Hammer 3rd, J. A., and X. S. Wu. 2002. Rabs grab motors: defining the connections between Rab GTPases and motor proteins. *Curr. Opin. Cell Biol.* 14:69–75.

59. Imamura, T., J. Huang, I. Usui, H. Satoh, J. Bever, and J. M. Olefsky. 2003. Insulin-induced GLUT4 translocation involves Protein Kinase C-l-mediated functional coupling between Rab4 and the motor protein kinesin. *Mol. Cell. Biol.* 23:4892–4900.

60. Bananis, E., S. Nath, K. Gordon, P. Satir, R. J. Stockert, J. W. Murray, and A. W. Wolkoff. 2004. Microtubule-dependent movement of late endocytic vesicles in vitro: requirements for dynein and kinesin. *Mol. Biol. Cell.* 15:3688–3697.

61. Tekotte, H., and I. Davis. 2002. Intracellular mRNA localization: motors move messages. *Trends Genet.* 18:636–642.

62. Jordens, I., M. Marsman, C. Kuijl, and J. Neefjes. 2005. Rab proteins, connecting transport and vesicle fusion. *Traffic.* 6:1070–1077.

63. Deneka, M., M. Neeft, and P. van der Sluijs. 2003. Regulation of membrane transport by Rab GTPases. *Crit. Rev. Biochem. Mol. Biol.* 38:121–142.

64. Tuvim, M. J., R. Adachi, S. Hoffenberg, and B. F. Dickey. 2001. Traffic control: Rab GTPases and the regulation of interorganellar transport. *News Physiol. Sci.* 16:56–61.

65. Sheff, D. R., E. A. Daro, M. Hull, and I. Mellman. 1999. The receptor recycling pathway contains two distinct populations of early endosomes with different sorting functions. *J. Cell Biol.* 145:123–139.

66. Sönnichsen, B., S. De Renzis, E. Nielsen, J. Rietdorf, and M. Zerial. 2000. Distinct membrane domains on endosomes in the recycling pathway visualized by multicolor imaging of Rab4, Rab5, and Rab11. *J. Cell Biol.* 149:901–914.

67. van der Sluijs, P., M. Hull, A. Zahraoui, A. Tavitian, B. Goud, and I. Mellman. 1991. The small GTP-binding protein Rab4 is associated with early endosomes. *Proc. Natl. Acad. Sci. USA.* 88:6313–6317.

68. Ullrich, O., S. Reinsch, S. Urbe, M. Zerial, and R. G. Parton. 1996. Rab11 regulates recycling through the pericentriolar recycling endosome. *J. Cell Biol.* 135:913–924.

69. van der Sluijs, P., M. Hull, P. Webster, P. Male, B. Goud, and I. Mellman. 1992. The small GTP-binding protein Rab4 controls an early sorting event on the endocytic pathway. *Cell.* 70:729–740.

70. Wu, X., B. Bowers, K. Rao, Q. Wei, and J. A. Hammer III. 1998. Visualization of melanosome dynamics within wild-type and dilute melanocytes suggests a paradigm for myosin V function in vivo. *J. Cell Biol.* 143:1899–1918.